NUMERICAL ANALYSIS OF BFRP REINFORCED CONCRETE SLAB EXPOSED TO IMPACT LOADS

Daniel Jindra and Petr Hradil

Brno University of Technology, Faculty of Civil Engineering, Institute of Structural Mechanics, Veveří 331/95, 602 00 Brno, Czech Republic; jindra.d@fce.vutbr.; hradil.p@fce.vutbr.cz

ABSTRACT

This paper describes advanced numerical analysis of a simply supported reinforced concrete slab exposed to close range explosion of a TNT charge. Finite element method (FEM) has been utilized in order to conduct the analysis. Non-linear material model for concrete slab is adopted. Reinforcing bars made of basalt fibre reinforced plastic (BFRP) are considered by elastic-plastic material model. 3D numerical model has been created, and a software with explicit solver (LS-Dyna) has been used in order to conduct analyses. A simplified modelling method of the blast loading has been utilized, which is based on the consideration of the load effects as a time dependent pressure. Several cases with different mesh size or different finite element formulation are investigated. The results are compared with experimental data based on study of fellow researchers. Match between the numerical analyses and measurements is discussed and considered as satisfying.

KEYWORDS

Impact loading, Concrete structure, Numerical analysis, Finite element model, Basalt fibre reinforced plastic (BFRP)

INTRODUCTION AND METHODS

Structures are required to retain its resistance also under severe loading conditions, while exposed to extreme loads, e.g. impacts of various objects. For example, air plane crash modelled by Králik [1], or impacts of projectiles (defence structures for military purposes). Structures are also required to withstand severe damage caused by pressure wave after explosion (different chemical explosives or gas explosion in civil structures). Several different approaches in modelling the effects of blast load are available in order to numerically analyse the response of exposed structures.

The simplest approach to model blast loading of a structure is to consider the pressure wave effects as a time dependent surface load. This approach has been also implemented in LS-Dyna [2], where it is described as "load blast enhanced" (LBE).

Another approach is Arbitrary Lagrangian Eulerian formulation (ALE), where the air domain surrounding the structure and the explosive material itself are included in the background multi material ALE mesh (MMALE) [2]. Blast pressure wave propagation through this environment is being modelled as well. Exposed structure is modelled by Lagrangian elements. Additionally, a fluid structure interaction needs to be established [2], in order to provide a constrain between ALE and Lagrangian meshes.

Coupling of the previous two approaches (LBE and ALE) is another option to consider blast loads. In this variant, the ALE mesh is established only in the closest structure surrounding. The exterior surface of the air domain which faces the blast (a layer of ambient elements [2]) is loaded by the empirical time dependent pressure function. The purpose of these ambient air elements in this edge layer is to convert the load pressure data into a thermodynamic state data, which are subsequently applied to the surrounding ALE air domain as a source. Density and particle velocity

are obtained from Rankine-Hugoniot relations [3]. Several comparative studies have been conducted, e.g. by Tabatabaei et al. [4], or Slavik [5], who compared mentioned methods.

The blast itself could also be modelled using a smooth particle hydrodynamics (SPH) method, which was presented by Monaghan and Lucy independently in 1977 [6,7]. This method has been utilized in large variety of tasks, e.g. by Schwer et al. [8] or Trajkovski [9], who modelled air blasts and compared SPH to previous methods.

Several concrete structures exposed to blast loading have been modelled, e.g. by Tai et al. [10]; Zhao and Chen [11,12], Thiagarajan et al. [13]; Dubec, Maňas, Štoller and Stonis [14]. In this study however, a numerical analysis of one of the physical experiments conducted by Feng et al. [15], who experimentally investigated the response of one-way concrete slab reinforced by basalt fibre reinforced plastic (BFRP) under close-in TNT explosion, has been conducted.

The main objective of this study is to compare the numerical analysis performance of a simply supported concrete slab loaded by a close-range explosion with data based on physical experiment [15] for 2 different mesh sizes and for three different finite element formulations, which are available to be utilized in the used FE software of LS-Dyna [2].

METHODS

In this study, the simplified approach of blast load has been adopted. The effect of the blast wave is considered as a time dependent pressure load applied at the exposed structure surface. This approach has been also implemented in LS-Dyna [2], where it is described as "load blast enhanced" (LBE). Closer details about these features are explained in subsequent chapters. Numerical finite element model has been created and explicit solver has been utilized to conduct the analyses.

For concrete slab, nonlinear material model proposed by Schwer and Murray [16] has been utilized. The parameter values of this model are based on the calibration study by Jiang and Zhao [17]. Basalt fibre reinforced plastic bars are considered with elastic-plastic material model.

PHYSICAL MODEL AND EXPERIMANTAL RESULT OF THE CONCRETE SLAB

The physical experiments are well described in the study by Feng et al. [15]. In this study, a variant of concrete slab noted as "B1-1" [15] is investigated. The concrete class of the slab is C40, with the average strength of concrete cubes cured for 150 days equal to 46.9 MPa [15]. The slab dimensions are: 1100 mm in length, 1000 mm in width, and 40 mm in height. Spacing (axial distance) of the BFRP bars is 50 mm in both directions, diameter is equal to Ø 6 mm. Concrete cover is equal to 5 mm, the effective depth of the slab is 32 mm.

The BFRP bars have been tested in order to establish the material properties [15]. The average tensile strength of 1.53 GPa, and the average elastic modulus of 57.68 GPa have been utilized as material values in this study. The shape of the TNT mass (200 g) is rectangular prism, located in the distance of 400 mm above the mid span of the slab upper surface. The slab is simply supported on a steel frame, with a structural span of 1000 mm. Strain gauges were pre-pasted onto the BFRP bars surface, two at the mid-span and two at the quarter span of the slab, as indicated in the Figure 1. The history of the axial strain of the BFRP bar (along the direction of the structural span) in the mid-span of the slab is depicted in the Figure 1.
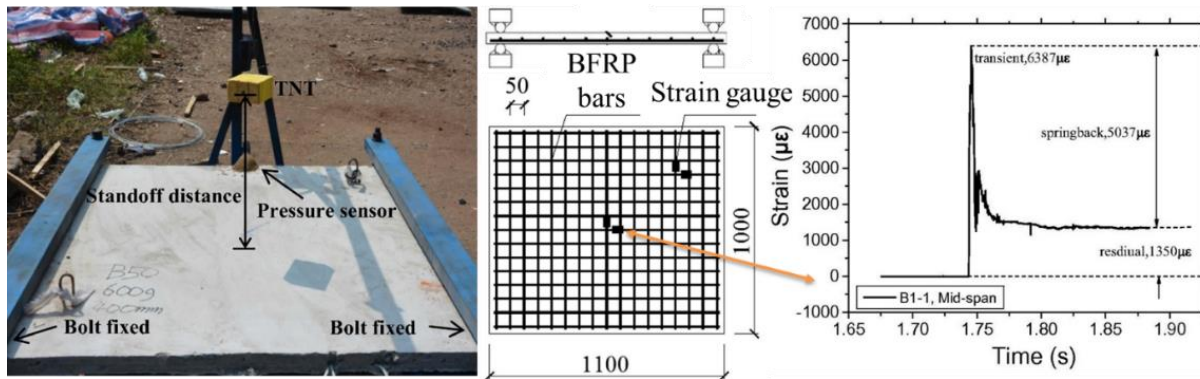
Fig. 1 – Experimental set-up and the mid-span strain history of the BFRP bar [15]

NUMERICAL ANALYSES

Modelling Approach of Blast Loading - Simplified Blast Model (LBE)

A simplified blast model with a pure Lagrangian approach of FEM is used in order to model the effect of a blast wave. The wave effect is considered as a time dependent pressure load, which is applied at the upper surface of the concrete slab, described as "load blast enhanced" (LBE) (LS-Dyna) [2]. It is based on the empirical blast loading function established by Randers-Pehrson and Bannister [18] defined as:

$$P(t) = P_r(t) \cos^2 \theta + P_s(t)(1 + \cos^2 \theta - 2\cos \theta) \tag{1}$$

where θ is the angle of incidence, $P_r(t)$ and $P_s(t)$ are time dependent reflected and incident overpressures respectively, both defined by Friedlander [19] equation. In case of $P_s(t)$ the function is defined as:

$$P_s(t) = P_{so} \left(1 - \frac{t}{t_o}\right) \cdot e^{-b\frac{t}{t_o}} \tag{2}$$

where P_{so} is the peak incident overpressure, b is a decay coefficient of the waveform, and to is the positive phase duration. These parameters are defined in dependence on scaled distance Z introduced by Hopkinson [20] and Cranz [21]:

$$Z = \frac{R}{W^{1/3}} \tag{3}$$

where R is the distance from the epicentre of blast, and W is the equivalent TNT mass. Parameter values in SI units are obtained from JRC report [22]. In this paper, the TNT mass is 200 g, located 400 mm above the upper surface mid span. The scaled distance Z is equal to $0.684 \ m \cdot kg^{-1/3}$. The arrival time of the blast wave is approximately 155 μs.

Material model for concrete - Schwer Murray Cap model

In order to describe the behaviour of the concrete slab, nonlinear material model needs to be utilized. Schwer Murray material model [16] is a material model suitable to analyse concrete structures, which is implemented in LS-Dyna material library [2] (MAT 145). The model is based on a yield surface defined by the function:

$$Y(I_1, J_2, J_3, \kappa) = J_2 - R(J_3)^2 F_f^{\ 2}(I_1) F_c(I_1, \kappa) \tag{4}$$

where I1 is the first invariant of the stress tensor. J2 and J3 are invariants of the deviatoric stress tensor. R(J3) is the Rubin strength reduction factor and κ is the cap hardening parameter. The yield surface consists of two parts: the hardening compaction surface $F_c(I_1, \kappa)$, and the shear failure surface $F_f(I_1)$ which is defined as:

$$F_f(I_1) = \alpha - \lambda \, e^{-\beta \, I_1} + \theta I_1 \qquad (5)$$

where parameters α, β, λ and θ are determined by triaxial compression test results. The expression of the hardening compaction surface is defined by equations:

$$F_c(I_1, \kappa) = 1 - \frac{(I_1 - L(\kappa))^2}{(X(\kappa) - L(\kappa))^2} \quad for \, I_1 > L(\kappa) \qquad (6)$$

$$F_c(I_1, \kappa) = 1 \quad for \, I_1 \leq L(\kappa) \qquad (7)$$

$$L(\kappa) = \kappa \quad for \, \kappa > \kappa_0 \qquad (8)$$

$$L(\kappa) = \kappa_0 \quad for \, \kappa \leq \kappa_0 \qquad (9)$$

$$X(\kappa) = L(\kappa) + RF_f(I_1) \qquad (10)$$

where R is the cap aspect ratio. Hardening compaction surface and the shear failure surface are combined by a multiplicative formulation which allows their continuous and smooth combination at their intersections.

Parameter values utilized for this material model are defined in accordance with the calibration study by Jiang and Zhao [17]. For this process, the uniaxial compression strength of f_{cm} = 46.9 MPa has been considered, which is the average strength of the test specimens as described by Feng et al. [15]. The values are summarized in the Figure 2.

1	MID	RO	SHEAR	BULK	GRUN	SHOCK	PORE	
	1	2400.0000	1.458e+10	1.944e+10	0.0	0.0	1.0	

2	ALPHA	THETA	GAMMA	BETA	EFIT	FFIT	ALPHAN	CALPHA
	1.372e+07	0.3292866	7.153e+06	2.460e-08	1.0000000	0.0	0.0	0.0

3	RO	XO	IROCK	SECP	AFIT	BFIT	RDAMO	
	2.0295680	1.058e+08	1	0.0	1.0000000	0.0018274	250.69104	

4	W	D1	D2	NPLOT	EPSMAX	CFIT	DFIT	TFAIL
	0.0650000	6.110e-10	2.225e-18	5.0000000	0.0	1.0000000	0.0036547	3.500e+06

5	FAILFG	DBETA	DDELTA	VPTAU				
	1	0.0	0.0	0.0				

6	ALPHA1	THETA1	GAMMA1	BETA1	ALPHA2	THETA2	GAMMA2	BETA2
	8.300e+05	0.0	2.407e+05	8.548e-09	7.600e+05	0.0	2.600e+05	7.411e-09

Fig. 2 – Material input card for MAT 145 (in SI units)

Numerical Finite Element Models

Numerical model geometry is based on the experimental model dimensions, and is depicted in the Fig. 3. The geometry of the steel frame supporting the slab is neglected, and simply supported slab is being modelled by utilizing the appropriate boundary conditions. The concrete slab consists of regular hexahedral mesh of solid elements (for 10 mm mesh in a shape of exact cubes). Reinforcing bars are modelled by beam elements with the same mesh size as the solid elements. Two variants of the mesh size are considered, 10 mm and 8 mm, with the total number of finite elements (solid + beam) equal to 48 610 (60 709 nodes) and 92 023 (110 901 nodes) respectively.
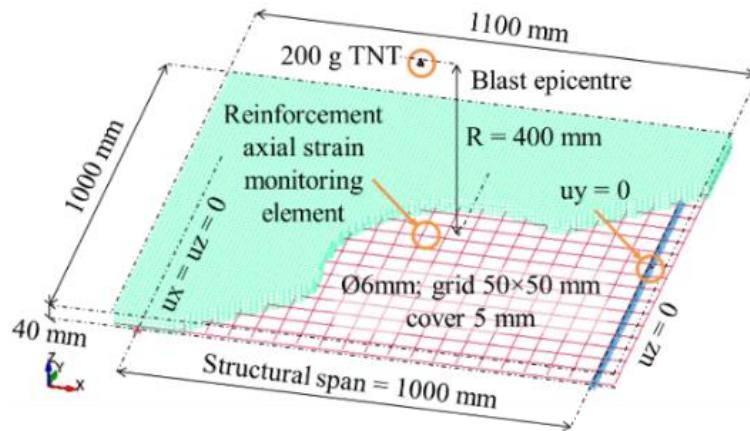
Fig. 3 – Numerical model geometry

Formulation of the beam elements is considered according to Hughes-Liu with cross section integration in all the cases. However various formulations of solid finite elements are adopted, noted as #A, #B and #C:

#A = Solid element with constant stress (along with hourglass control) (option "1" in LS-Dyna [2])
#B = Fully integrated solid intended for poor aspect ratio elements (efficient formulation, option "-1" in LS-Dyna [2])
#C = Fully integrated solid [2] (option "2" in LS-Dyna [2])

The history of axial strain is being monitored in a reinforcing bar located in the mid-span of the slab, in the direction of the structural span (x direction of the GCS).

Reinforcement material (BFRP) has been considered as bilinear material model with negligible hardening, practically linear elastic and ideal plastic behaviour. Material values are based on experimental tests [15], described in the chapter 1 of this study.

ANALYSES RESULTS

Figure 4 depicts the first principal strain at the bottom and top surface of the concrete slab in various times of the numerical analysis. History of axial strain of the reinforcement bar in the mid-span (along the structural length of the slab) is plotted in the Fig. 5 for several cases (as described in the previous chapter), along with the measured reference approximation. This reference is obtained graphically from the picture in Figure 1 right [15].
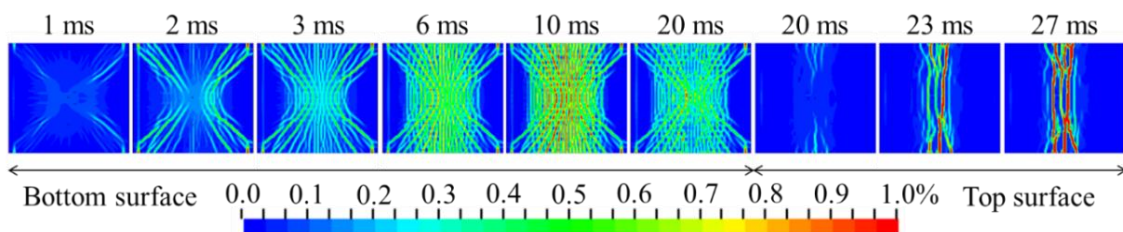

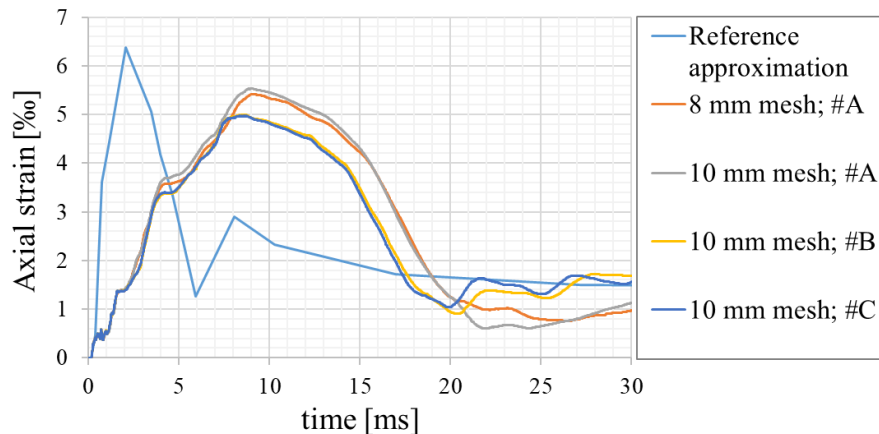*Fig. 4 – First principal strain plots at the top and bottom slab surface in various time (#A, 10 mm mesh)*

Fig. 5 – History of axial strain in the reinforcement bar.

DISCUSSION

Two mesh sizes have been compared so far, 10 and 8 mm grid. The difference in the results is rather negligible (Figure 5). Coarser mesh has not been investigated, as it is assumed, that for 40 mm thick slab, 10 mm mesh is already coarse enough. More significant difference in the analysis result is observed, when a different solid element formulation has been adopted. For cases with full integration (#B and #C), the maximal axial strain values in the steel bar are 5.0‰, whereas for the single point integration (#A), the peak strain is approx. 5.5‰. The initial strain rate (slope of the graph) is slightly smaller than the reference approximation in all the cases (Figure 5). In order to see this difference more precisely, direct experimental data would be required rather than graphically approximated curve. The axial strain maximums of all the modelled cases (5.0 - 5.5 ‰) are in good match with the measured peak (6.4‰). It is assumed that in order to obtain better match in strain rate (slope of the strain-time curve), the stiffness of the numerical model is required to be calibrated. It is not expected the finer mesh or a different material models (for concrete) would have significant influence on the initial strain rate [23].

The crack patterns at the bottom surface of the concrete slab have developed in the direction parallel to the supports, and also in diagonal directions (Figure 6 right). The first principal strain plots (Figure 4 left part) are of similar patterns. More significant upper surface cracks have evolved in the direction parallel to the slab supports (Figure 6 left). The same patterns are observed in the first principal strains (Figure 4 right part), which were caused by the slab oscillations initiated by the dynamic load.

Fig. 6 – Damage patterns of the slabs after physical experiment at top surface (left) and bottom surface (right) [15].

The simplified blast model considers the spherical source of the explosion from a single point [2], with the validity range of scaled distance Z in interval $(0.147; 40)\ m \cdot kg^{-1/3}$. The scaled distance value of the experiment set up is $0.684\ m \cdot kg^{-1/3}$, therefore within the validity interval of the

simplified blast approach. However, the shape of the TNT explosive was not spherical (but rectangular prism), what might cause some additional differences between the experimental and numerical results.

CONCLUSION

Explicit finite element numerical analyses (FEA) of the simply supported concrete slab reinforced with basalt fibre reinforced plastic (BFRP) have been conducted. The structure is exposed to a pressure wave caused by a close-range blast of 200 g TNT.

Three different formulations of the concrete solid elements, here referred as #A, #B and #C have been considered. The formulations differed in integration point numbers or other modifications.

Two densities of the mesh have been considered, regular 8 mm and 10 mm mesh of the concrete solid elements. Finer meshes have not been investigated yet. Significant differences in the results of analysed models and possible finer mesh models are not expected. However, computational time would be rapidly increased, hence the number of elements was kept below 125 000 to optimize the performance of the analyses. The difference in the results (crack patterns, axial strain) between 8 mm and 10 mm meshes is also rather negligible. It is assumed that slightly finer mesh would be more suitable (5 mm) in order to capture the concrete crack patterns more precisely, and yet sustain reasonable computational time. This will be tested in the subsequent research studies.

Based on the observed axial strain in the reinforcement bar, the results of the numerical analyses and the experimental data are in a nice match considering the maximums of the strain-time curves, with 5.0 - 5.5 ‰ for numerical analyses and 6.4 ‰ for the experiment. However, the strain rates (slopes of the strain history curves) obtained from the numerical analyses are noticeably smaller than the strain history based on experimental data (Figure 5). Although the reference strain-time data are based on a graphical approximation of raster figure (Figure 1), the approximation error is expected to be smaller than this difference.

Performance of a different material model (for concrete) has not yet been examined for this current setting. Various material models consider strain rate effects slightly differently, and it is possible some might be more suitable. Moreover, the structure stiffness (along with boundary condition stiffness) itself might have significant influence and would require certain calibration. These features could be crucial for a proper strain rates of the reinforcement bar. Further investigation is required.

ACKNOWLEDGEMENTS

REFERENCES

[1]   Králik, J. (2014). Safety of nuclear power plant against the aircraft attack. Applied Mechanics and Materials, vol. 617, p. 76 – 80. ISSN: 1662-7482. DOI: 10.4028/www.scientific.net/AMM.617.76.

[2]   Livermore Software Technology Corporation (1997), LS-Dyna® Theoretical Manual. Livermore, CA: Livermore Software Technology Corporation.

[3]   Kinney, G. F., Graham K.J. (1985). Explosive shocks in Air. Springer-Verlag Berlin Heidelberg. Online ISBN: 978-3-642-86682-1, 1985. DOI: 10.1007/978-3-642-86682-1.

[4]   Tabatabaei, Z.S., Volz J.S. (2012). A comparison between three different blast methods in LS-Dyna®: LBE, MM-ALE, Coupling of LBE and MM-ALE. Paper presented at the 12th International LS-Dyna® Users Conference, Detroit U.S. 2012.

[5]   Slavik, T. (2010). A coupling of empirical explosive blast loads to ALE air domains in Ls-Dyna®. Paper presented at the 7th European LS-Dyna® Conference, Salzburg Austria 2009.

[6] Gingold R.A., Monaghan J.J. (1977). Smoothed particle hydrodynamics: theory and application to non-spherical stars. Monthly Notices of the Royal Astronomical Society vol. 181, is. 3, p. 375–389, ISSN (online): 1365-2966. DOI: 10.1093/MNRAS/181.3.375.

[7] Lucy L.B. (1977). A numerical approach to the testing of the fission hypothesis. The Astronomical Journal, vol. 82, p. 1013–24. ISSN: 00046256. DOI: 10.1086/112164.

[8] Schwer, L., Hailong T., Mhamed, S., (2015). LS-Dyna Air Blast Techniques: Comparisons with Experiments for Close-in Charges. Paper presented at the 10th European LS-Dyna® Conference, Würzburg Deutschland 2015.

[9] Trajkovski J. (2017). Comparison of MM-ALE and SPH methods for modelling blast wave reflections of flat and shaped surfaces. Paper presented at the 11th European LS-Dyna® Conference, Salzburg Österreich 2017.

[10] Tai, Y.S., Chu T.L., Hu H.T. and Wu J.Y. (2011). Dynamic response of a reinforced concrete slab subjected to air blast load. Theoretical and Applied Fracture Mechanics. vol. 56, issue. 3, pages.140–147. ISSN 0167-8442. DOI: 10.1016/j.tafmec.2011.11.002.

[11] Zhao, C.F., Chen J.Y. (2013). Damage mechanism and mode of square reinforced slab subjected to blast loading. Theoretical and Applied Fracture Mechanics. vol. 63-64, p. 54-62. ISSN 0167-8442. DOI: 10.1016/j.tafmec.2013.03.006.

[12] Zhao, C.F., Chen J.Y., Wang Y. and Lu S.J. (2012). Damage mechanism and response of reinforced concrete containment structure under internal blast loading. Theoretical and Applied Fracture Mechanics. vol. 61, p. 12-20. ISSN 0167-8442. DOI: 10.1016/j.tafmec.2012.08.002.

[13] Thiagarajan, G., Kadambi A.V., Robert S. and Johnson C.F. (2015). Experimental and finite element analysis of doubly reinforced concrete slabs subjected to blast loads. International Journal of Impact Engineering. vol. 75, p. 162-173. ISSN 0734-743X. DOI: 10.1016/j.ijimpeng.2014.07.018.

[14] Dubec, B., Maňas P., Štoller J. and Stonis P. (2019). Experimental and numerical assessment of fibre reinforced concrete slab under blast load, ICMT 2019 - 7th International Conference on Military Technologies, Proceedings 2019. ISBN: 978-172814593-8. DOI: 10.1109/MILTECHS.2019.8870129.

[15] Feng, J., et al. (2017). Experimental research on blast-resistance of one-way concrete slabs reinforced by BFRP bars under close-in explosion. Engineering Structures, vol. 150 p.550-561. ISSN: 0141-0296. DOI: 10.1016/j.engstruct.2017.07.074.

[16] Schwer, L.E., Murray Y.D. (1994). A three invariant smooth cap model with mixed hardening. International Journal for Numerical and Analytical Methods in Geomechanics, vol. 18, pp. 657-688, DOI: 10.1002/nag.1610181002.

[17] Jiang, H., Zhao J. (2015). Calibration of the continuous surface cap model for concrete, Finite Elements in Analysis and Design. vol. 97, p. 1-19. ISSN 0168-874X. DOI: 10.1016/j.finel.2014.12.002.

[18] Randers-Pehrson, G., and Bannister K.A. (1997). Airblast loading model for DYNA2D and DYNA3D. Army Research Laboratory, Rept. ARL-TR-1310, U.S., 1997.

[19] Friedlander, F.G. (1946). The diffraction of sound pulses I. Diffraction by a semi-infinite plane. Proceedings of the Royal Society A. 1946. ISSN 0080-5630. DOI: 10.1098/rspa.1946.0046.

[20] Hopkinson, B., (1915) British Ordnance board minutes 13565, in: The National Archives, Kew, UK, pp.11.

[21] Cranz, C., (1925) Lehrbuch der Ballistik. Erster Band. AusereBalistik, Springer Verlag, Berlin.

[22] Karlos, V., Solomos G. (2013). Calculation of blast loads for application to structural components. JRC Technical Reports, Report EUR 26456 EN, Luxembourg. ISSN 1831-9424. DOI: 10.2788/61866.

[23] Jindra, D., Hradil P., Kala J., Král P. (2020). Mesh size influence of the concrete slab FE model exposed to impact load for various material models. Transactions of VSB - Technical University of Ostrava, Civil engineering Series, 20(2), 1-7, DOI: 10.35181/tces-2020-0010.